ACS Macro Letters

Letter

pubs.acs.org/macroletters

Spatially Resolved Concentration and Segmental Flow Alignment in a Shear-Banding Solution of Polymer-Like Micelles

A. Kate Gurnon,[†] Carlos López-Barrón,[§] Matthew J. Wasbrough,[†,‡] Lionel Porcar,[∥] and Norman J. Wagner*,[†]

[†]Center for Neutron Science, Department of Chemical & Biomolecular Engineering, University of Delaware, Newark, Delaware 19716, United States

[‡]Center for Neutron Research, National Institute of Standards and Technology, Gaithersburg, Maryland 20899, United States

[§] ExxonMobil Chemical Company, Baytown, Texas 77520-2101, United States

[∥]Institut Laue-Langevin, BP 156, F-38042 Grenoble Cedex 9, France

Supporting Information

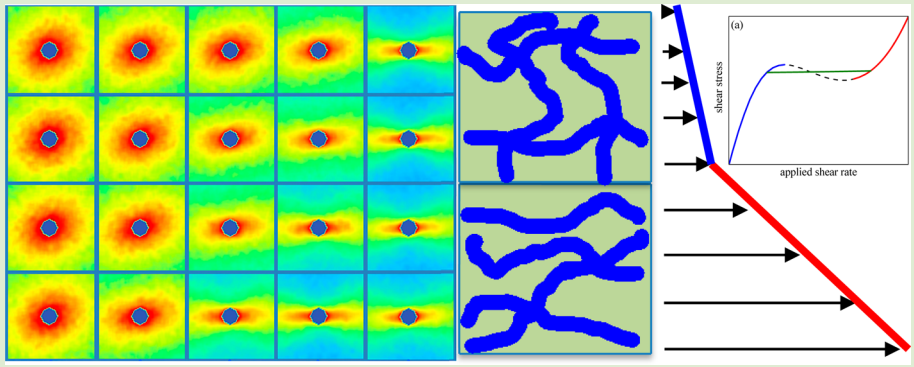

ABSTRACT: We measure the spatially resolved microstructure and concentration in the plane of flow for a viscoelastic solution of polymer-like micelles comprised of mass fraction 6.0% (volume fraction 6.6%) solution of 2:1 molar ratio cetylpyridinium chloride/sodium salicylate in 0.5 mol/L NaCl/D_2O through the shear banding transition. Spatially resolved flow small-angle neutron scattering measurements in the velocity−velocity gradient (1−2) plane of flow establish the local microstructure, and scanning narrow-aperture flow ultrasmall-angle neutron scattering (SNAFUSANS) measurements indicate no flow-induced concentration gradients within measurement accuracy. These results show shear banding in this solution is not associated with an isotropic−nematic transition and are fundamentally important for validating models of shear-banding complex fluids. Improvements in the SNAFUSANS method are also documented.

The mechanism for shear banding in worm-like or polymer-like micelles (WLM, PLM) and its theoretical description remain a well-studied and controversial topic since the seminal work of Rehage and Hoffman over 20 years ago.[1,2] The shear-banding rheology for a wide variety of worm-like micellar surfactant systems has been studied over a range of topologies from relatively short, rigid micelles[3−5] to long, thread-like micelles[6−9] and branching leading to supramolecular networks.[10,11] In its simplest form, shear banding is observed as the coexistence of a high and low shear band in the velocity−velocity gradient (1−2) plane of flow as identified by flow-velocimetry measurements.[8,9,12]

The search for the physical origin of shear banding is motivated by theory coupling the shear-induced alignment and fluctuation of polymers to the nonlinear rheology.[13] Indeed, for surfactant and polymer systems, such flow instabilities are thought to be *intrinsic* to the material itself.[14] A shear-banding instability is predicted for a nonmonotonic rheological constitutive equation (RCE) with an unstable region, where stress decreases with increasing shear rate.[15] The physical reasons for this unstable regime in the RCE include extreme shear thinning, such as observed in the classical Doi−Edwards[16] or Giesekus[5] models for polymer rheology, shear-induced phase separations,[17] and more recently, shear-induced micellar breakage.[18,19]

Numerous cationic worm-like micellar systems have been shown by rheo-SANS measurements to exhibit shear banding concurrent with a shear-induced nematic phase transition.[3−6,20,21] Of significance is the observation that, for these relatively short, strongly interacting PLMs, shear banding occurs in close proximity to the equilibrium isotropic−nematic phase transition, and importantly, shear banding is accompanied by significant concentration gradients between the

Received: January 8, 2014
Accepted: February 25, 2014
Published: March 4, 2014

   dx.doi.org/10.1021/mz5000152 | *ACS Macro Lett.* 2014, 3, 276−280

bands. Indeed, the development of a new experimental sample geometry that enables spatially resolved ultrasmall angle neutron scattering afforded the first quantitative measurements of shear-induced concentration gradients.[3] The method of scanning narrow-aperture ultrasmall-angle neutron scattering (SNAFUSANS) uses a sealed, horizontally mounted Couette geometry and a highly collimated neutron beam to accurately measure the transmission under shearing flow within the different velocity bands coexisting in a shear-banding complex fluid. Neutron transmissions are a direct measure of chemical compositions. These results, coupled with flow-SANS measurements of the spatially resolved flowing microstructure, provided the first, quantitative nonequilibrium phase diagram for a shear-banding PLM.[4] Therein, the formation of a nematic phase with low viscosity as the high shear band is accompanied by surfactant concentration enrichment at the expense of the nearly isotropic, high viscosity surfactant solution comprising the low-shear band. This enrichment is comparable to that observed at equilibrium, and thus, a shear-induced isotropic−nematic phase transition leading to shear banding is found to be tightly tied to the underlying equilibrium phase behavior. SNAFUSANS measurements are reported here to resolve the controversy in the literature concerning the underlying mechanism for the observed shear banding in a different model system comprised of a long, entangled thread-like micellar system.

It is relevant that other worm-like surfactant solutions comprised of long, but *highly branched*, worm-like micelles also exhibit shear banding, but this is a consequence of a completely different shear-induced phase separation that is itself localized to the high shear band.[11] Shear-induced demixing is observed for compositions in proximity of a phase separation characterized by equilibrium between a dense, highly branched gel coexisting with a dilute brine phase.[10] Comparison between these very different mechanisms of shear banding for these two extreme micellar topologies indicates that direct measurements of the local microstructure and surfactant concentration are necessary and warranted to properly establish the mechanism underlying the nonlinear material instability. This is especially relevant as results for the PLM solutions under consideration here may also provide insight into the nonlinear polymer rheology.[15,22−25]

Theoretical predictions for concentration coupling accompanying shear banding generally take one of three possible forms (for a review, see ref 22). For rheological constitutive equations where a decreasing stress is predicted for increasing shear rates, a mechanical instability under shear flow can manifest as shear banding.[13,15,26] Steady shear banding can occur without any concentration gradients; however, an additional criterion is needed for selection of the stress in the plateau region, such as afforded by stress diffusion.[27] When flow-induced concentration fluctuations[28] are significant, flow alignment of the microstructure leads to a lower viscosity and enhanced diffusion of the PLM (or polymer) toward the less-aligned, more viscous material.[17] This shear extension and disentanglement of polymers drive diffusion *up* concentration gradients toward the concentrated, entangled region and lead to coupling of concentration gradients with the mechanical instability.[22] Lastly, a shear-induced nematic transition generates a low viscosity nematic phase in coexistence with a high viscosity entangled, nearly isotropic fluid. This latter mechanism leads to the *opposite* concentration gradient as for the former case as the nematic phase is inherently more concentrated than the viscous, isotropic phase.[17,21,29,30] To date, only the latter case of a concentration gradient toward the high shear band has been definitively measured, and this was for compositions in the close vicinity of an equilibrium isotropic−nematic transition.[3] Here, in this work we investigate concentration−flow coupling in a highly entangled, thread-like micellar fluid system far from any equilibrium phase transition using the novel USANS transmission measurements with spatial resolution under steady shear flow.[3]

Berret and co-workers extensively studied the shear rheology of the model PLM system under investigation here up to the isotropic−nematic (I−N) transition.[17,31] A characteristic plateau in the stress−shear rate curve was interpreted as a first-order transition between a viscous isotropic phase in the low shear band coexisting with a shear-induced nematic state. With decreasing surfactant concentration, the plateau in the stress was observed to be less pronounced, and the authors suggested the transition becomes second-order. However, no quantitative measurements of the microstructure or local concentrations in the banding state were reported. Through comparison to flow-SANS measurements on a related system by Schmitt et al.[32] and work on other PLM solutions known to undergo an I−N transition under flow,[20] they proposed shear banding is due to the formation of a nematic phase. Indeed, for more concentrated solutions than those studied here (mass fraction 10%) NMR measurements have been interpreted to show a nematic-like alignment in the high shear band.[25] This interpretation of shear banding driven by an I−N transition for this system was critiqued by Hu and Lips,[8] who performed detailed velocimetry and small-angle light scattering measurements under flow. Working on a similar composition (mass fraction 7.3% 2:1 ratio in 0.5 M NaCl, but in H_2O) as studied here, they concluded that the shear banding resulted from the coexistence of entangled and disentangled regions of PLMs and not the shear-induced nematic transition.[8,9]

Here we resolve the discrepancy in the literature concerning the mechanism of shear banding in viscoelastic, linear PLM solutions by direct measurements of the microstructure and concentration during shear flow for a well-characterized solution comprised of (volume fraction 6.6%) solution of 2:1 molar cetylpyridinium chloride/sodium salicylate in 0.5 mol/L NaCl in D_2O.[33,34] A typical Maxwellian linear viscoelastic behavior is observed in Figure S1 (Supporting Information (SI)).[35] Figure 1 shows the nonlinear shear rheology for the PLM solution measured in a standard Couette geometry (ARES, TA Instruments), where a stress plateau is evident across a broad range of applied shear rates. This is a signature of shear banding and is verified by independent velocimetry measurements.

Figure 1 shows representative small-angle neutron scattering (SANS) measurements at selected spatial positions across the velocity gradient direction and applied shear rates for the velocity−velocity gradient (1−2) experimental geometry (I vs q plots are in the SI).[36] The shear-induced anisotropy in the scattering patterns is indicative of the significant flow alignment of the PLMs, where stronger alignment is observed closer to the inner rotating cylinder and lesser alignment near the other stationary wall for nominal shear rates corresponding to the stress plateau. These direct microstructural measurements clearly show evidence of structural differences coexisting within the flow field that indicates shear banding and can be further quantified by an alignment factor, A_ϕ and ϕ_0 is the principle axis of the scattering relative to the flow direction, using standard

dx.doi.org/10.1021/mz5000152 | ACS Macro Lett. 2014, 3, 276−280

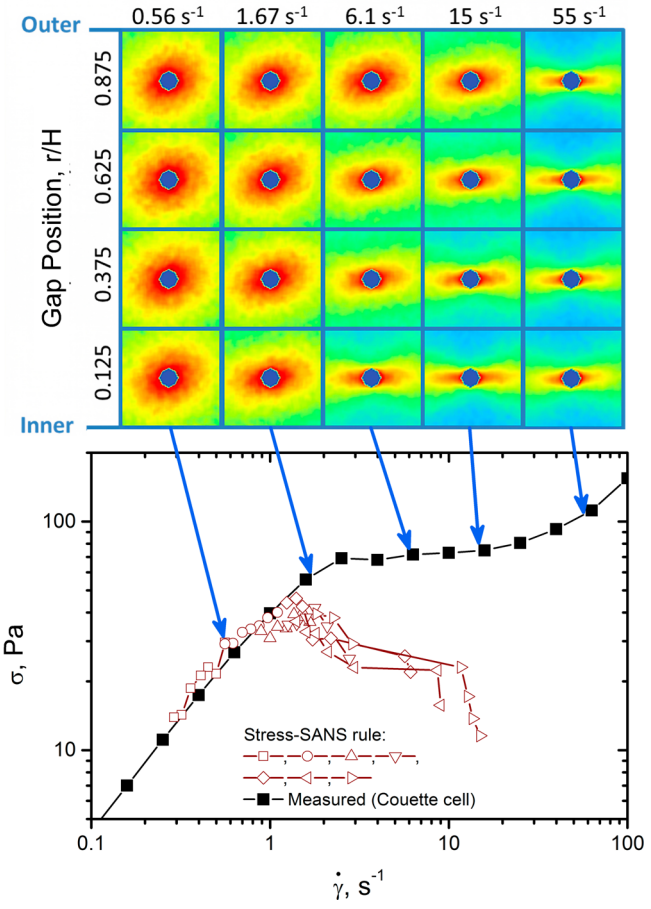

Figure 1. Top: SANS patterns at representative gap positions and nominal shear rates as indicated. Bottom: measured shear stress versus nominal shear rate and the calculated shear stresses from analysis of the SANS patterns, velocimetry measurements, and the stress-SANS rule (see Supporting Information).

methods.[5,11,37] Figure 2 shows that A_f and ϕ_0 follow the trends as observed visually in the SANS patterns, where the results are now plotted against the local shear rates obtained from velocimetry. The critical values for $A_{f,1c}$ (0.09) and $\phi_{0,1c}$ (22.8°) at the onset of shear banding as reported by Helgeson et al.[5] for a system comprised of shorter, more rigid micelles are also indicated in the figure and are in good agreement with those reported here. Note that although flow alignment is observed, which is in agreement with previous flow-NMR[12] and flow-birefringence measurements[6] on related samples, the alignment factor never exceeds ~0.4, which is significantly lower than that expected and observed for a nematic phase.[5]

Figure 3 shows the measured transmissions (top) and the calculated surfactant volume fractions (bottom) as a function of spatial location across the velocity-gradient direction of shear for the nominal shear rates indicated. To within measurement accuracy, the transmissions are constant across the gap of the Couette for all shear rates. The local surfactant concentrations calculated from these transmissions are found to be constant to within measurement accuracy across the gap for all applied shear rates. The SNAFUSANS methodology and sources of uncertainty are discussed further in the SI. As a check of reproducibility, a scan was performed at rest after the highest shear rate (open black symbols in Figure 3). Comparison with the initial scan at rest (closed black symbols) provides a direct measure of precision. Another measure of precision in volume fraction, which is used to set the confidence interval (±0.013), is the variation in repeated, independent transmission measurements performed in 5 mm thick demountable SANS cells at rest (see SI Figure S3). The transmissions for the final rest state were used to determine the difference in concentration under flow for each slit position. Further, as mass is conserved within the cell, the variation of the average volume fraction from the rest value can also be taken as a measure of accuracy, although we are not able to sample directly adjacent to the cell walls. Nonetheless, the largest deviation in average concentration is ~2% in volume fraction (Figure S5, SI), and this is for the highest shear rate tested. The largest of these three values of measurement precision is of the surfactant concentration, and therefore, we conclude that no shear-induced concentration changes are evident to within this level of precision. Thus, no significant concentration gradient of surfactant is evident in the shear-banded states for this PLM solution.

The new SNAFUSANS measurements show that no significant concentration differences are created during shear

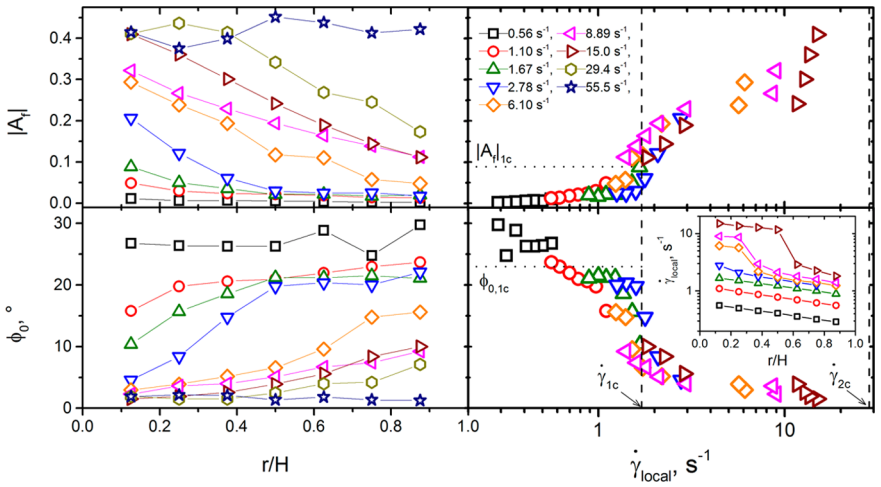

Figure 2. (Left) Top: alignment factor. Bottom: orientation angle (principle axis of scattering) as a function of the relative gap position for the nominal shear rates. (Right) Top: alignment factor. Bottom: orientation angle versus the local shear rate in the flow cell (inset shows the local shear rates).

dx.doi.org/10.1021/mz5000152 | ACS Macro Lett. 2014, 3, 276−280

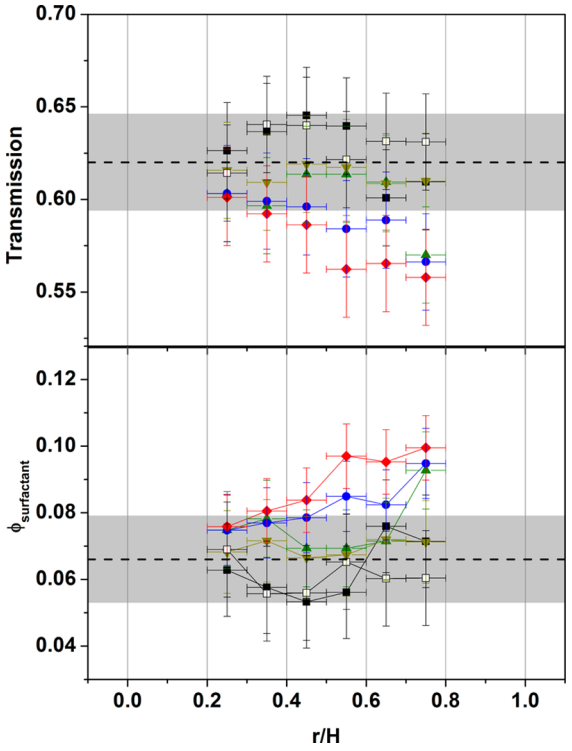

Figure 3. (Top) transmission. (Bottom) surfactant volume fraction, versus relative gap position for shear rates (s^{-1}) initial 0 (black ■), 0.56 (dark green ▲), 2.2 (light green ▼), 22 (blue ●), 56 (red diamond), final 0 (white □). The confidence interval is indicated by a shaded area around the initial quiescent volume fraction ($\phi(\dot{\gamma} = 0) = 0.066 \pm 0.013$) and transmission ($T(\dot{\gamma} = 0) = 0.062 \pm 0.026$).

banding; this observation is in direct contrast to what would be expected if a nematic state forms in the high shear band. Both the absence of a measurable concentration enhancement and the comparatively low segmental alignment in the high shear band as compared to that for a nematic fluid support the conjectures of Hu and Lips concerning the underlying mechanism of shear banding in this highly entangled, thread-like micellar solution:[8] that the steady-shear banded state is the coexistence of a flow-aligned, low-viscosity (low entanglement density) PLM in the high shear band with a highly entangled, viscoelastic PLM in the low shear band. Recent spatiotemporal resolved 1−2 flow-SANS measurements confirm the proposed mechanism during startup of shear flow.[34] Importantly, these results clearly show that the alternative hypothesis,[38] that nucleation and growth of a nematic phase near the inner rotating wall drives shear banding, is not observed for this composition. This is not surprising given the relative distance in composition space between the sample and the equilibrium I−N transition (mass fraction ∼23%). Berret shows that the shear banding rheology is more extreme for higher surfactant concentrations, and further research along the lines developed here is warranted to determine at what concentration the proximity to the I−N transition plays a role in shear banding[31] and further instabilities.[23]

As noted in previous[8] and recent work[34] on this PLM, strong flow, small-angle light scattering butterfly patterns are also observed for this sample in the high shear band. These patterns are a signature of longer length scale concentration fluctuations[28] characteristic of shear-induced demixing.[10,39] The rheological consequences of these shear-induced concentration fluctuations are addressed by recent studies of the transient shear-flow behaviors of this system.[33,34] Finally, whether this coupling plays a role in setting the intrinsic material instability or whether micellar scission[19] is relevant is a current topic of investigation that includes direct comparison of these new, quantitative results for the microstructure and local concentration with advanced constitutive models.

■ ASSOCIATED CONTENT

Supporting Information

Linear viscoelasticity, SANS and SNAFUSANS (methods, calibration, data, and data analysis), scattering intensity versus q, and velocimetry data. This material is available free of charge via the Internet at http://pubs.acs.org.

■ AUTHOR INFORMATION

Corresponding Author

*E-mail: wagnernj@udel.edu.

Notes

The authors declare no competing financial interest.

■ ACKNOWLEDGMENTS

This manuscript was prepared under cooperative agreements 70NANB7H6178, 70NANB10H256, and 70NANB12H239, from NIST, U.S. Department of Commerce. The statements, findings, conclusions, and recommendations are those of the author(s) and do not necessarily reflect the view of NIST or the U.S. Department of Commerce. We acknowledge F. Nettesheim, M. Helgeson, and T. Hu for the particle tracking velocimetry measurements.

■ REFERENCES

(1) Rehage, H.; Hoffmann, H. *J. Phys. Chem.* **1988**, *92* (16), 4712−4719.
(2) Rehage, H.; Hoffmann, H. *Mol. Phys.: Int. J. Interface Chem. Phys.* **1991**, *74* (5), 933−973.
(3) Helgeson, M. E.; Porcar, L.; Lopez-Barron, C.; Wagner, N. J. *Phys. Rev. Lett.* **2010**, *105*, 8.
(4) Helgeson, M. E.; Reichert, M. D.; Hu, Y. T.; Wagner, N. J. *Soft Matter* **2009**, *5* (20), 3858−3869.
(5) Helgeson, M. E.; Vasquez, P. A.; Kaler, E. W.; Wagner, N. J. *J. Rheol.* **2008**, *53* (3), 727−756.
(6) Cappelaere, E.; Berret, J. F.; Decruppe, J. P.; Cressely, R.; Lindner, P. *Phys. Rev. E* **1997**, *56* (2), 1869−1878.
(7) Cappelaere, E.; Cressely, R.; Decruppe, J. P. *Colloids Surf., A* **1995**, *104* (2−3), 353−374.
(8) Hu, Y. T.; Lips, A. *J. Rheol.* **2005**, *49* (5), 1001−1027.
(9) Hu, Y. T.; Palla, C.; Lips, A. *J. Rheol.* **2008**, *52* (2), 379−400.
(10) Thareja, P.; Hoffmann, I. H.; Liberatore, M. W.; Helgeson, M. E.; Hu, Y. T.; Gradzielski, M.; Wagner, N. J. *J. Rheol.* **2011**, *55* (6), 1375−1397.
(11) Liberatore, M. W.; Nettesheim, F.; Wagner, N. J.; Porcar, L. *Phys. Rev. E* **2006**, *73* (2), 020504.
(12) Fischer, E.; Callaghan, P. T. *Phys. Rev. E* **2001**, *64* (1), 011501.
(13) Spenley, N. A.; Cates, M. E.; McLeish, T. C. B. *Phys. Rev. Lett.* **1993**, *71* (6), 939−942.
(14) Goddard, J. D. *Annu. Rev. Fluid Mech.* **2003**, *35*, 113−133.
(15) Olmsted, P. D. *Rheol. Acta* **2008**, *47* (3), 283−300.
(16) Cates, M. E.; McLeish, T. C. B.; Marrucci, G. *Europhys. Lett.* **1993**, *21* (4), 451−456.
(17) Schmitt, V.; Marques, C. M.; Lequeux, F. *Phys. Rev. E* **1995**, *52* (4), 4009−4015.
(18) Vasquez, P. A.; McKinley, G. H.; Cook, L. P. *J. Non-Newtonian Fluid Mech.* **2007**, *144* (2−3), 122−139.

(19) Germann, N.; Cook, L. P.; Beris, A. N. *J. Non-Newtonian Fluid Mech.* **2013**, *196*, 51−57.
(20) Berret, J. F.; Roux, D. C.; Lindner, P. *Eur. Phys. J. B* **1998**, *5* (1), 67−77.
(21) Schmitt, V.; Lequeux, F.; Pousse, A.; Roux, D. *Langmuir* **1994**, *10* (3), 955−961.
(22) Cates, M. E.; Fielding, S. M. *Adv. Phys.* **2006**, *55* (7−8), 799−879.
(23) Lerouge, S.; Berret, J. F. Shear-Induced Transitions and Instabilities in Surfactant Wormlike Micelles. In *Polymer Characterization: Rheology, Laser Interferometry, Electrooptics*; Dusek, K., Joanny, J. F., Eds.; Springer: New York, 2010; Vol. *230*, pp 1−71.
(24) Hu, Y. T. *J. Rheol.* **2010**, *54* (6), 1307−1323.
(25) Boukany, P. E.; Wang, S. Q. *Macromolecules* **2008**, *41* (4), 1455−1464.
(26) Dhont, J. K. G.; Briels, W. J. *Rheol. Acta* **2008**, *47* (3), 257−281.
(27) Lu, C. Y. D.; Olmsted, P. D.; Ball, R. C. *Phys. Rev. Lett.* **2000**, *84* (4), 642−645.
(28) Helfand, E.; Fredrickson, G. H. *Phys. Rev. Lett.* **1989**, *62* (21), 2468−2471.
(29) Fielding, S. M.; Olmsted, P. D. *Eur. Phys. J. E* **2003**, *11* (1), 65−83.
(30) Olmsted, P. D.; Lu, C. Y. D. *Phys. Rev. E* **1999**, *60* (4), 4397−4415.
(31) Berret, J. F.; Roux, D. C.; Porte, G. *J. Phys. II* **1994**, *4* (8), 1261−1279.
(32) Grand, C.; Arrault, J.; Cates, M. E. *J. Phys. II* **1997**, *7* (8), 1071−1086.
(33) Gurnon, A. K.; Lopez-Barron, C.; Eberle, A. P. R.; Porcar, L.; Wagner, N. J. *Soft Matter* **2014**, DOI: 10.1039/c3sm53113a.
(34) Lopez-Barron, C.; Gurnon, A. K.; Eberle, A. P. R.; Porcar, L.; Wagner, N. J. *Phys. Rev. E* **2014**, submitted.
(35) Cates, M. E.; Candau, S. J. *J. Phys.: Condens. Matter* **1990**, *2* (33), 6869−6892.
(36) Kline, S. R. *J. Appl. Crystallogr.* **2006**, *39*, 895−900.
(37) Walker, L. M.; Wagner, N. J. *Macromolecules* **1996**, *29* (6), 2298−2301.
(38) Berret, J. F. *Langmuir* **1997**, *13* (8), 2227−2234.
(39) Fielding, S. M.; Olmsted, P. D. *Phys. Rev. E* **2003**, *68*, 3.